Journal of Neuroscience Methods 146 (2005) 98–105

JOURNAL OF NEUROSCIENCE METHODS

www.elsevier.com/locate/jneumeth

A method to measure the strength of multi-unit bursts of action potentials

Brian Mulloney *

Neurobiology, Physiology and Behavior, 196 Briggs Hall, University of California Davis, Davis, CA 95616-8519, USA

Received 5 August 2004; received in revised form 26 January 2005; accepted 26 January 2005

Abstract

Both the numbers of neurons that are active during multi-unit bursts of spikes and the frequencies with which individual neurons fire in these bursts can vary in response to changes in excitation. Here is a digital-filtering method that measures the strength of a burst of spikes by calculating the area of a polygon derived from the squared voltages that record the burst, and dividing this area by the burst's duration. The method was developed in the SigmaPlot© environment, and makes use of the Fast-Fourier Transform functions provided in the SigmaPlot© transform language. To test the method's performance, I constructed multi-unit bursts of spikes with known structure and calculated the strengths of these known bursts. To demonstrate the method's usefulness, I applied it to a train of 23 bursts of spikes in motor axons recorded during a spontaneous bout of patterned motor output. The measured strengths of these bursts varied 30-fold, and were well-correlated with the differences in the original recording. The results demonstrate that the method effectively measures burst strength independent of burst duration.

Keywords: Burst strength; Firing frequency; Excitation; Motor pattern

1. Introduction

Recordings from many neurophysiological experiments include simultaneous bursts of action potentials in many neurons. During an experiment, the numbers of neurons firing and the frequencies with which they fire can vary spontaneously and in response to experimental manipulation. Temporal features of these bursts like duration or period are straightforward to measure from recordings of voltages and times, but quantitative changes in numbers of units recruited and their firing frequencies are often more difficult to measure. In the laboratory, we often speak of strong and weak bursts because visual inspection of the recordings and aural monitoring of the recording during the experiment lead to the intuitive sense that bursts can vary in "strength". How can we measure this intuitive parameter when the numbers of active units and their individual firing frequencies are unknown?

The amplitude of spikes recorded with an extracellular electrode in a restricted extracellular space is proportional to the diameter of the axon, whether the electrode configuration is monophasic or triphasic (Pearson et al., 1970). Units with larger diameter axons have larger spikes, a feature that is apparent in many motor systems where recruitment of motor units proceeds in order of size. I sought a method that would sum the activity of all the neurons that fired during a burst, taking into account both spike frequency and spike amplitude. In the past, analog rectification and integration of bursts has been useful under some circumstances (e.g. Mulloney et al., 1987; McClellan and Hagevik, 1997), but these methods tended to confound firing frequency and burst duration. I have developed a digital-filtering method that takes a recorded train of bursts, isolates each burst, and calculates an area proportional to the numbers and sizes of spikes and to the burst's duration. If the burst's duration is known independently, this area can be divided by this duration to create a measure of burst strength, that is, the numbers and sizes of spikes that occurred during the burst.

* Tel.: +1 530 752 1110; fax: +1 530 752 5582.
E-mail address: bcmulloney@ucdavis.edu.

0165-0270/$ – see front matter © 2005 Elsevier B.V. All rights reserved.
doi:10.1016/j.jneumeth.2005.01.020

I describe the method and the logic behind it, demonstrate its performance on synthetic bursts of spikes with known composition, and apply it to an experimental recording of bursts that varied in intensity but whose detailed composition was unknown.

2. Methods

2.1. Physiological data

We isolated the abdominal ventral nerve cord from crayfish, *Pacifastacus leniusculus*, using procedures that are described in Tschuluun et al. (2001). Action potentials were recorded extracellularly from either the first segmental nerve (N1) of abdominal ganglion A3 or A4 (Mulloney and Hall, 2000), or from the superficial branch of the third segmental nerve (N3) of these ganglia (Kennedy and Takeda, 1965). We used pin electrodes in a triphasic configuration for N1 recordings and suction electrodes for N3 recordings (Pearson et al., 1970; Stein and Pearson, 1971). High-gain amplification and band-pass filtering (0.3–5 kHz) of these recordings was conventional. Recordings were saved as computer files in abf format by digitizing the amplifiers' output at 100 μs sampling rate using an Axon Instruments Digidata 1200B board and Axoscope software (Axon Instruments, Foster City, CA). The selected recordings were imported into SigmaPlot© using the DataAccess plug-in (Bruxton Corp., Seattle, WA).

2.2. Test data

To construct bursts of spikes with known composition, I used a single spike recorded from N3, duplicated it repeatedly, and scaled these duplicates to create trains of spikes with specified frequencies and specified sizes. In bursts with five "units", the largest unit was five times the size of the smallest unit. Spike frequencies in these bursts conformed to the size principle known to govern the orderly recruitment of motor units in crayfish and other animals (Davis, 1971); the smallest unit fired at the highest frequency, the largest at the lowest frequency. The numbers of spikes per second for each unit was varied systematically to create bursts with low (range 17–5 Hz), medium (range 61–17 Hz), and high (range 97–57 Hz) levels of firing; these corresponded to different levels of excitation in a real motor pool.

These bursts were constructed by first creating a list of time–voltage pairs the length of one cycle period that matched the sample-frequency of the original spike. All voltage values in this list were initially zero. For each unit, the scaled list of voltages derived from the single spike was then added periodically to the voltages in the new list, starting at times specified by the firing frequency of that unit. This method allowed units whose spikes overlapped in time to sum algebraically, as do real spikes in multi-unit recordings.

3. Description of the method for measuring areas of burst envelopes

This method for measuring the intensity of bursts begins with paired lists of times and voltages (t, V) that describe a recording, organized in two columns. These lists are then processed in four steps:

1. The list of voltages (V) is squared. This operation makes all values positive or zero.
2. The list of squared voltages (V^2) is then smoothed to create a continuous envelope whose height is proportional to local values of V^2.
3. Values of this smoothed envelope smaller than a threshold value are clipped out by setting them to zero; other values are unchanged. Given an appropriate choice of threshold, this isolates a polygon corresponding to each burst.
4. The area of each polygon is calculated. This area is a measure of intensity times duration.
5. If the duration of each burst is known independently, dividing the area of each burst by its duration gives a measure of burst intensity, or strength, independent of burst duration.

The different features of this procedure are discussed next.

3.1. Smoothing

V^2 is highly irregular, and the boundaries of each burst are not well-enough defined to permit algorithmic identification. In order to define bursts as opposed to individual spikes, it is necessary to smooth V^2. The choice of a smoothing procedure is a crucial feature of this method. I tested several different low-pass smoothing filters, including both time-domain boxcar filters and frequency-domain filters, and found the most effective to be one provided with SigmaPlot©, the "Smoothing transform". This is a procedure that transforms V^2 to the frequency domain, filters it there using a triangular smoothing kernel, and restores the result to the time domain. Hamming (1977) describes the logic behind these FFT filters and discusses the choice of filtering kernels. This procedure is by comparison very fast, and does not generate bogus humps in the output that would confound the calculation of areas associated with each burst.

This smoothing procedure makes use of several functions provided in the SigmaPlot© transform language, and requires seven steps:

1. The list of V^2 values is transformed into the frequency domain using the FFT function.
2. A "triangular smoothing kernel" is constructed. The width of this kernel determines how many neighboring points will be considered in calculating the value that will replace each raw data point in the smoothed list, and weights these neighboring points by their distance from the data point.
3. The "triangular smoothing kernel" is transformed to the frequency domain using the FFT.

```
                    ' Input
                         ' Import t, V from abf file into col 1 and col 2
Times = 1                ' Column with times from recording
V = 2                    ' Column with voltages from recording
SV2 = 3                  ' Column 3 will get smoothed squared voltages
Envelope = 4             ' Column 4 will get clipped Envelope of each burst

n = 500                  ' Sets width of triangular smoothing kernel

Xbar = 0                 ' Should be 0.4 * Mean of unsmoothed V squared;
                         ' set to 0 if you want to calculate it here.
thfrac = 0.375           ' Fraction of Mean to use calculating threshold
                         ' Empirically, 37.5% of mean defines bursts nicely

                    ' Procedure adapted from SigmaPlot's 's "SMOOTHING.xfm"
x = col(V) * col(V)      ' Square the voltages to rectify them.
n1 = size(x)
tx = fft(x)              ' fft of squared data
nx = size(tx)/2

                         ' generate triangular smoothing kernel
lt = {data(n,0,-1), data(0,0,nx-2*n-2), data(0,n)}
lt1 = lt/total(lt)
tk = fft(lt1)            ' fft of kernel
td = mulcpx(tk,tx)       ' convolve kernel and data
sd = invfft(td)          ' transform back to time domain
tsd = real(sd)           ' recover real components of complex results

                    ' Output
                         ' strip out padded channels created by FFT
ru = if(mod(n1,2)>0, (nx-n1+1)/2, (nx-n1+2)/2)
rl = if(mod(n1,2)>0, nx-ru, nx-ru+1)
tsd1 = tsd[data(ru,rl)]
col(SV2) = tsd1          ' save smoothed data to worksheet

                         ' Zero smoothed voltages less than threshold.
If Xbar = 0 then         ' This isolates polygons of individual bursts.
    thresh = mean(col(SV2)) * thfrac
else
    thresh = Xbar * thfrac
end if
                         ' Clip out the tiny voltages, and save the rest.
col(Envelope) = If(col(SV2) < thresh, 0, col(SV2))
```

Fig. 1. The procedure, written the SigmaPlot© transform language, that smoothes the recorded voltages and isolates a polygon in V^2 whose area is proportional to the intensity and duration of each burst in the recording. The "FFT" and "INVFFT" functions compute the Fourier transform and inverse Fourier transform of V^2 and adjust them to the required dimensions. The "triangular smoothing kernel" established the relative weights given to local values of V^2 in the smoothing process. The final conditional statement compares each value of V^2 to a threshold criterion, and zeros it if it is smaller than the threshold.

4. The kernel and the transformed data are convolved using a function for multiplication of matrices of complex numbers.
5. The product of this convolution is transformed back to the time domain using an inverse-FFT function.
6. The real numbers in the complex output of the inverse-FFT operation are saved in a new column of the SigmaPlot© spreadsheet.
7. The smoothed V^2 are examined and values less than a specified threshold are set to zero.

This procedure smoothes V^2 and clips out the smallest values of V^2 to create polygons corresponding to each burst. These polygons are defined as sequential lists of (t, V^2) that are separated by zeros in the V^2 column.

The first parameter that the user must consider is the width of the smoothing kernel, which is defined by the parameter "n" in Fig. 1. A broader kernel makes a smoother burst envelope, but too broad a kernel will obscure the boundaries of bursts. The sampling rate used to digitize the original recording is also a major determinant of the appropriate value for this parameter. In the experimental data I used to develop and test this method, an individual triphasic spike lasted 5 ms and was sampled every 100 μs, so each digitized spike was described by 50 points in (t, V). I experimented with n = 250, 500, and 1000, which correspond to kernels 50 ms, 100 ms, and 200 ms wide, and found that n = 500 gave the best definition of the envelopes of individual bursts. Raw data sampled at other rates would require tuning of this parameter.

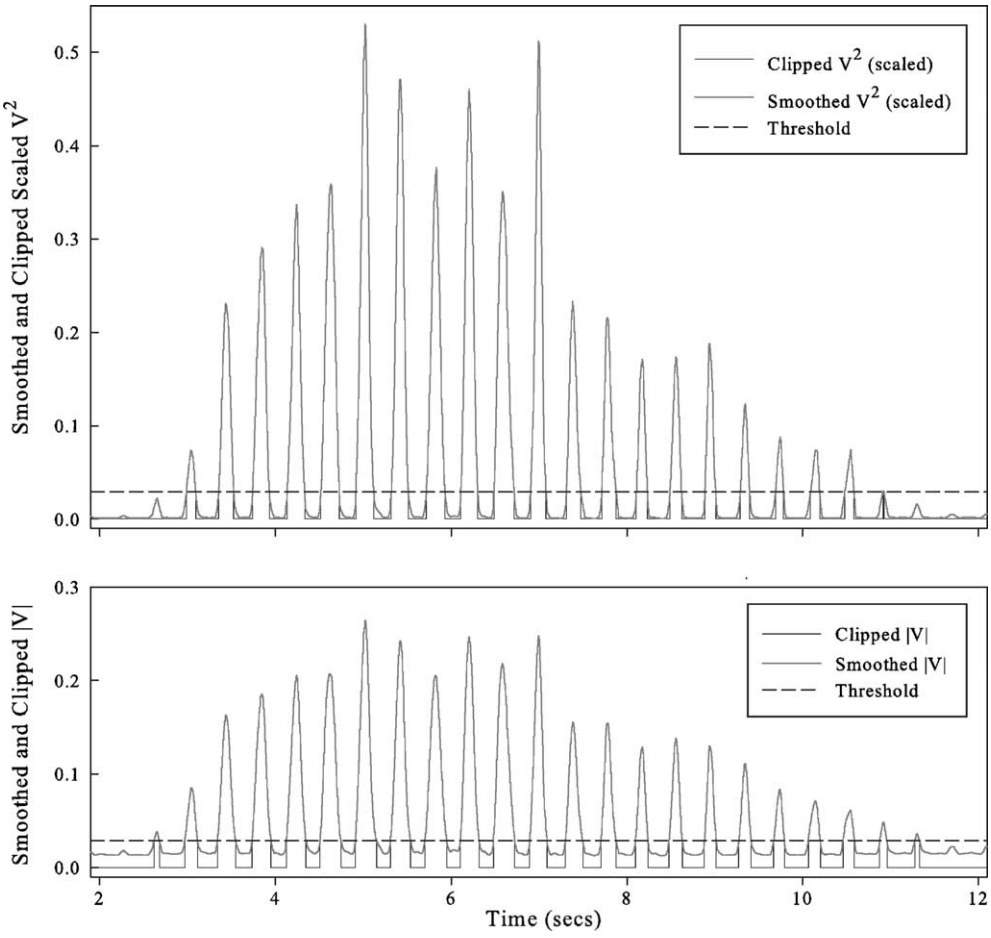

Fig. 2. Comparison of the smoothed burst envelopes created using V^2 and $|V|$ of the same recording. To permit accurate visual comparison, the V^2 data were scaled so that their mean value was identical to that of the $|V|$ data. The dimensions and scaling of the axes of these two plots are identical, and the threshold is drawn at the same value in each.

3.2. Defining the areas of individual bursts

The second parameter that must be specified is the threshold for clipping the smoothed V^2. Once the data have been smoothed, this threshold is used to isolate the polygon for each burst. For clean recordings, I found values of 0.375 times the mean of the list of smoothed V^2 to be effective; noisier recordings require higher thresholds. The result of this procedure is a smoothed and clipped list of V^2 that retains its association with the list of times. Zeros in the list of V^2 are considered to be outside the bursts.

In SigmaPlot©, it is straightforward to check the performance of the smoothing parameter and a given threshold by plotting the smoothed V^2 and clipped V^2 as functions of time, superimposed in different colors.

3.3. Why V^2 as opposed to $|V|$

The decision to square V rather than to use the absolute value of V has two benefits. It emphasizes the large values associated with each spike, and minimizes the values recorded between spikes. Provided the error is less than 1 V, this minimization also reduces the effect of any constant bias introduced by a dc offset in the recording amplifier. To compare the results of these two alternatives, I used the same parameters to smooth V^2 and $|V|$, scaled the smoothed V^2 to the same mean as the smoothed $|V|$, and plotted the two curves on the same axes (Fig. 2). Even though the mean values of the scaled V^2 and $|V|$ are identical, the smoothed V^2 curve comes closer to zero between each burst, which allows the use of a lower threshold for defining individual bursts.

3.4. Calculating the area of each burst's envelope

To isolate each burst, the next procedure (Fig. 3) reads down the list of clipped V^2 to find values that are not zero. Upon encountering a non-zero V^2, it saves this value and its associated time in a new pair of lists and does so with each subsequent pair of (t, V^2) until the next zero is reached, which marks the end of that burst. It then uses the SigmaPlot© "area" function to calculate the area of the polygon from this new list of paired time, V^2 values. The "area" function has a feature with important consequences; it handles polygons like these that are not closed (the first time is different from

```
Times = 1                       ' Column with times from recording
Envelope = 4                    ' Column with clipped Envelopes of bursts
StartTime = Envelope + 1        ' Column to hold Time at which each burst began
Areas = Envelope + 2            ' Column to hold Area of each burst' envelope
Scratch = Envelope + 3
                                ' Now find the area of each burst's envelope
cell(Scratch, 1) = 1                ' row to list x, y
cell(Scratch, 2) = Envelope + 4     ' column to start list of y values
cell(Scratch, 3) = 1                ' row index for results

for i = 1 to size(col(Envelope)) do
   k = cell(Scratch, 1)             ' row index
   j = cell(Scratch, 2)             ' col index
   m = cell(Scratch, 3)

   if cell(Envelope,i) > 0 then     ' This is part of an envelope

      cell(  j, k) = cell(Times, i)
                                    ' Subtracting thresh removes DC offset
      cell(j+1, k) = cell(Envelope, i) - thresh

      if cell(Envelope,i + 1) > 0 then
          cell(Scratch, 1) = cell(Scratch, 1) + 1
      else
                                    ' The burst is finished, so calculate
                                    ' its Area, save its StartTime, and
                                    ' increment the results indecies
          cell(StartTime, m) = cell(j, 1)
          cell(Areas, m) = Area(col(j), col(j + 1))

          cell(Scratch, 1) = 1      ' Shift to next column for next burst
          cell(Scratch, 2) = cell(Scratch, 2) + 2
          cell(Scratch, 3) = cell(Scratch, 3) + 1
      end if
   end if
end for
```

Fig. 3. This procedure examines the list of smoothed and clipped V^2 to identify and isolate the pairs of time, V^2 values that enclose each smoothed burst. As it marches through the list, it saves the time at which each burst's envelope begins and the area of its envelope.

the last time) by closing the polygon with a line from the first point to the last before calculating the area. Thus, only values above the threshold are included in the area calculated for each burst; any dc offset recorded along with the data is excluded.

The procedure saves both the time at which each polygon began and its area as a separate list. This list of start-times can then be used to associate each area with other parameters of individual bursts measured with different techniques (Mulloney and Hall, 1987).

4. Results

To test the performance of this method, I constructed nine bursts that contained spikes from five different units. These bursts had durations of 0.2, 0.5, or 0.8 s (Fig. 3). For each duration the firing frequencies within the bursts were low, medium, or high. These bursts of spikes resembled natural bursts produced in response to weak, moderate, or strong excitation (Davis, 1971; Mulloney, 1997).

Using the procedure described above, I transformed and smoothed these bursts and calculated the areas of the resulting polygons. The smoothed envelope of each burst is plotted over the burst itself in Fig. 4. The areas of these envelopes grow rapidly as burst duration and firing frequencies increase (Fig. 5A). Notice that the duration of each envelope is at best an approximation of the duration of the burst from which it was generated.

The area of each polygon is influenced both by the numbers of spikes that occur and by the burst's duration. By dividing each of these areas by the measured duration of the burst, we calculate a parameter that reflects the firing frequencies and sizes of the units active during the burst — the strength of the burst (Fig. 5B). In these constructed bursts, there were always five units and each unit fired at low, medium, or high frequencies, so I would expect to see three similar levels of strength independent of burst duration. This is what occurred (Fig. 5B).

To test the usefulness and sensitivity of this method, I applied it to a recording of a spontaneous bout of activity in the pool of motor neurons that innervate power-stroke muscles of one crayfish swimmeret (Mulloney and Hall, 2000). During this bout, the numbers of spikes per unit and the number of units recruited during each burst waxed and waned (Fig. 6). The different components of this figure illustrate the trans-

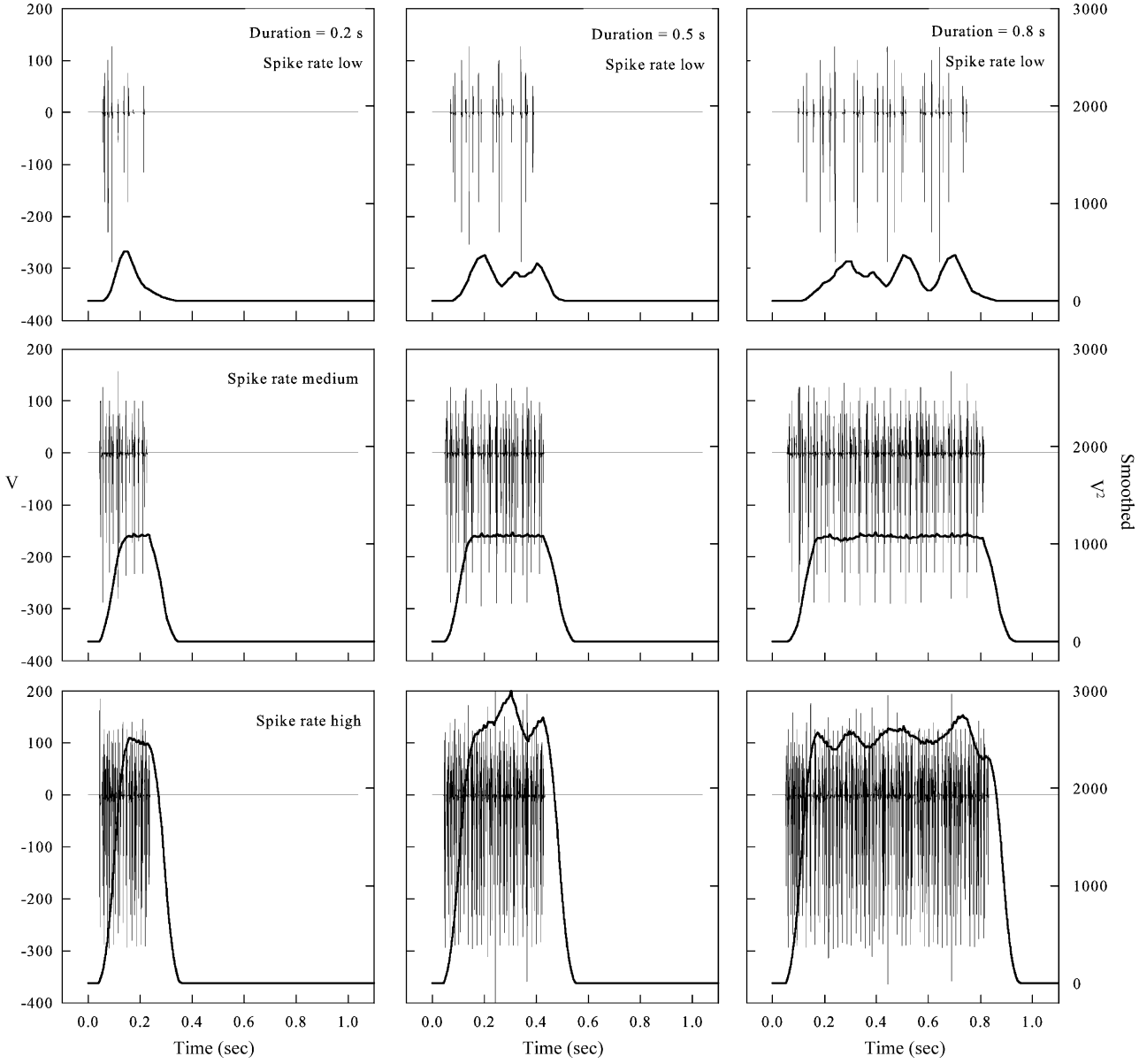

Fig. 4. Nine bursts of spikes, each with five units, and their transformation into polygons whose areas are a measure of burst intensity and duration. These bursts differ in duration (0.2, 0.5, or 0.8 s) and in the firing frequencies of each unit (low, medium, or high).

formation of the raw data (Fig. 6A) to V^2 (Fig. 6B) and to the smoothed envelope of V^2 (Fig. 6C). Finally, the normalized strengths of these bursts are plotted as functions of the time at which each burst began (Fig. 6A).

The descriptive statistics of the raw voltages in this recording, the smoothed V^2, and the clipped V^2 were affected mostly by the squaring step. The mean ± S.D. of original raw voltages (-0.0969 ± 0.0982), the smoothed V^2 (0.0097 ± 0.0223), and the clipped V^2 (0.0094 ± 0.0224) differed most notably in sign. In contrast, the areas of the 23 polygons had a mean ± S.D. = 0.5853 ± 0.4579 and ranged from 1.3490 to 0.0133. The burst strengths had a mean ± S.D. = 0.3365 ± 0.1983, and ranged from 0.6716 to 0.0229, a 30-fold difference. These different values of strength correspond well to the differences apparent in the original recording (Fig. 6A).

4.1. Normalization of burst strengths

In practice, the absolute size of each recorded spike will be affected by the gain and filters of the preamplifier and by the extent of the extracellular restriction (Stein and Pearson, 1971), which will affect the calculated area of a burst's envelope. In many circumstances, we want to describe changes in burst strength rather than absolute strength, and as long as the configuration of the electrode and recording system

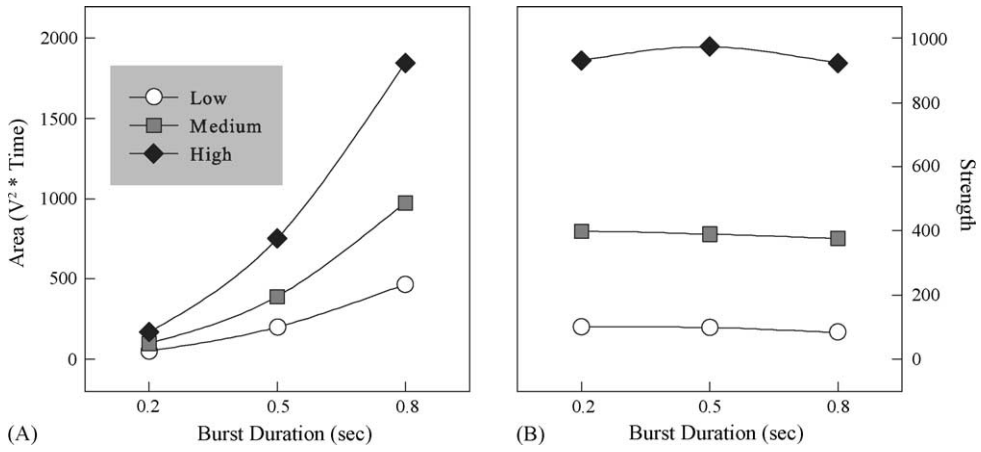

Fig. 5. (A) The areas of each smoothed burst increased as spike frequencies increased and as burst duration increased. (B) Burst strength was measured by dividing the area of each burst by its duration, which yielded a metric sensitive to the numbers and sizes of spikes in the burst but independent of the burst's duration.

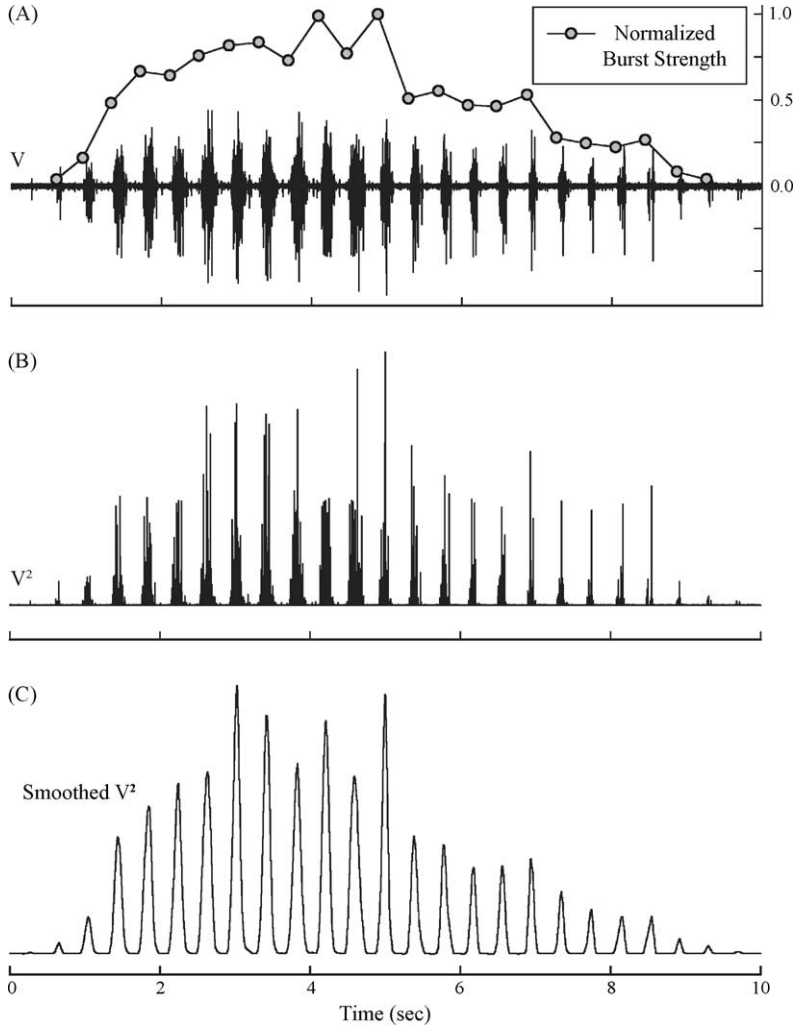

Fig. 6. An episode of activity in a swimmeret motor nerve that illustrates spontaneous changes in burst strength. (A) The original recording of voltage (V) as a function of time. The circles show the relative strength of each burst, plotted at the time the burst started. (B) The squared voltages (V^2) plotted on the same time axis. (C) The result of processing V^2 with the smoothing algorithm (smoothed V^2) described in Section 2, plotted on the same time axis.

are unchanged, an effective way to do so is to normalize the calculated strengths to the largest recorded strength, creating a range from zero to one. This normalization is illustrated in Fig. 6A.

5. Discussion

This method provides a reliable and effective method to measure the relative strengths of bursts of spikes in a train of recorded activity. The method makes intuitive sense because the sizes of the recorded spikes reflect the flux of charges across cell membranes during the action potentials (Stein and Pearson, 1971), and captures both the sizes of different units and the numbers of spikes they fire. In situations where each spike in each unit can be counted, other measures of their activity are also informative (Namba and Mulloney, 1999). However, this method demands neither knowledge of the numbers of units that are active nor the ability to separate their spikes, and so is useful for the many situations where resolution of each unit is impossible.

The correction of the measured areas of polygons by duration is an important feature because it separates low-intensity from high-intensity bursts that have similar areas (Fig. 5). In the examples shown in Figs. 5 and 6, I measured the duration of each burst independently, and so could confidently make this correction. In cases where the duration of each burst is uncertain, the user might use the duration of each polygon as an estimate of the true burst duration.

This method was developed in the SigmaPlot© environment using the SigmaPlot© transform language. Clearly, it can be applied in any environment that provides functions for FFT, inverse-FFT, and multiplication of complex matrices. The only additional requirement is the ability to import experimental recordings.

Acknowledgements

I thank Daniel Coleman for providing the original recording of the spike used to construct the bursts, and Trish Harness for providing the recording in Fig. 6. This research was supported by grants NSF IBN 0091284 and USPHS NINCDS NS 048149.

References

Davis WJ. Functional significance of motoneuron size and soma position in swimmeret system of the lobster. J Neurophysiol 1971;34:274–88.
Hamming RW. Digital filters. Englewood Cliffs, NJ: Prentice-Hall; 1977.
Kennedy D, Takeda K. Reflex control of abdominal flexor muscles in the crayfish. II. The tonic system. J Exp Biol 1965;43:229–46.
McClellan AD, Hagevik A. Descending control of turning locomotor activity in larval lamprey: neurophysiology and computer modeling. J Neurophysiol 1997;78:214–28.
Mulloney B. A test of the excitability-gradient hypothesis in the swimmeret system of crayfish. J Neurosci 1997;17:1860–8.
Mulloney B, Hall WM. The PD programs: a method for the quantitative description of motor programs. J Neurosci Methods 1987;19:47–59.
Mulloney B, Hall WM. Functional organization of crayfish abdominal ganglia: III. Swimmeret motor neurons. J Comp Neurol 2000;419:233–43.
Mulloney B, Acevedo LD, Bradbury AG. Modulation of the crayfish swimmeret rhythm by octopamine and the neuropeptide proctolin. J Neurophysiol 1987;58:584–97.
Namba H, Mulloney B. Coordination of limb movements: three types of intersegmental interneurons in the swimmeret system and their responses to changes in excitation. J Neurophysiol 1999;81:2437–50.
Pearson KG, Stein RB, Malhotra SK. Properties of action potentials from insect motor nerve fibers. J Exp Biol 1970;53:299–316.
Stein RB, Pearson KG. Predicted amplitudes and form of action potentials recorded from unmyelinated nerve fibers. J Theor Biol 1971;32:539–58.
Tschuluun N, Hall WM, Mulloney B. Limb movements during locomotion: tests of a model of an intersegmental coordinating circuit. J Neurosci 2001;21:7859–69.